Inorganic Chemistry
Article
Cite This: Inorg. Chem. 2018, 57, 10616−10624
pubs.acs.org/IC

Multiferroism in Iron-Based Oxyfluoride Perovskites

Steven T. Hartman,*[,†] Sung Beom Cho,[‡] and Rohan Mishra*[,†,‡]

[†]Institute of Materials Science and Engineering and [‡]Department of Mechanical Engineering and Materials Science, Washington University in St. Louis, St. Louis, Missouri 63130, United States

Supporting Information

ABSTRACT: Multiferroic materials with simultaneous magnetic and ferroelectric ordering that persist above room temperature are rare. Using first-principles density functional theory calculations, we demonstrate fluorination of oxygen-deficient $AA'Fe_2O_5$ perovskites, where A and A' are cations with +3 and +2 oxidation states, respectively, and have a layered ordering, as an effective strategy to obtain room-temperature multiferroics. We show that by controlling the size of the A and A' cations, it is possible to stabilize a noncentrosymmetric phase arising due to the hybrid improper ferroelectricity mechanism, with polarization as high as 13 $\mu C/cm^2$. The fluorination also stabilizes Fe in +3 oxidation state, which results in superexchange interactions that are strong enough to sustain magnetic order well above room temperature. We also show the presence of a magnetoelectric coupling wherein the switching mode that reverses the direction of the spontaneous polarization also affects the strength of the magnetic interactions. The results show that low-temperature fluorination of anion-deficient perovskites with layered cation ordering can be an effective approach to design new multiferroics.

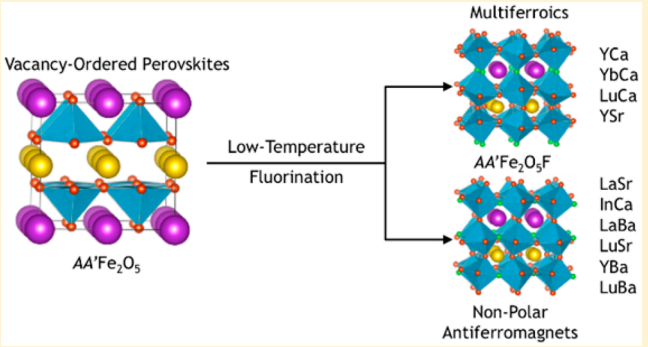

INTRODUCTION

Transition-metal oxides with the AMO_3 perovskite framework, where A is a larger cation and M is a smaller transition-metal cation, display a wide range of physical phenomena such as high-temperature superconductivity,[1] giant magnetoresistance,[2,3] and high ionic conductivity.[4,5] The perovskite framework is a three-dimensional network of corner-connected MO_6 octahedra with the larger A cations occupying cuboctahedral cavities between the octahedra. These MO_6 octahedra can distort or undergo cooperative tilts,[6,7] so the perovskite framework is flexible enough to accommodate a wide variety of elements from the periodic table.[8] Substitution of additional cations sharing the same sites can tune existing functionalities, or even induce new ones, especially when combined with layer-by-layer-growth techniques, such as molecular beam epitaxy, to produce cation ordering.[9−11] This strategy is well illustrated in the class of multiferroic perovskites that have simultaneous electric polarization and magnetism. Magnetism usually originates due to transition-metal cations with partially filled d-orbitals, while the conventional ferroelectric mechanism, seen in perovskites such as $BaTiO_3$, requires B-site cations with empty d-orbitals.[12] This constraint can be lifted to achieve multiferroism by selecting two different cations, one for each task. For instance, in $EuTiO_3$, magnetism arises due to the unpaired f-electrons of Eu, while the $3d^0$ Ti cation undergoes polar distortion.[13] In $BiFeO_3$, polarization arises due to the steric hindrance of the $6s^2$ lone-pair electrons of Bi,[14] while the $3d^5$ electrons of Fe^{3+}undergo magnetic ordering. In the family of hybrid improper ferroelectrics, the layered ordering of two cations at the A-site, when coupled with the correct combination of octahedral tilts, results in a finite polarization.[15−18] This is because the tilts lead to displacement of A-site cations along opposite directions in successive layers, but if the two A-site cations do not have identical size or charge, the resulting dipoles do not cancel completely, leaving a net polarization, as shown in Figure 1. This polarization can, in principle, be switched by changing the direction of octahedral tilting.[19,20] Since the ferroelectricity in this case results from the A-site cations, the B-site cations can have magnetic moments due to occupied d-orbitals.

Substitution of a second anion having different size and charge is emerging as another promising route to control perovskite properties.[21−23] For example, fluorination of a thin film of $SrFeO_{3-\delta}$ reduced the film's electrical resistance by 5 orders of magnitude,[24] and fluorination of $NdNiO_3$ changed it from a metal to a semiconductor with 2.1 eV band gap.[25] In $La_{0.7}Ca_{0.3}MnO_{3-\delta}F_x$, fluorination to x = 0.6 increased the ferromagnetic Curie temperature from 258 to 269 K, while also raising the metal−insulator transition temperature by 16 K.[26] Substitution with nitride has also been shown to affect the band gap,[27] electric polarity,[28] and photocatalytic properties;[29] however, anion substitution has not yet been used to create a room-temperature multiferroic.

Received: May 7, 2018
Published: August 14, 2018

DOI: 10.1021/acs.inorgchem.8b01253
Inorg. Chem. 2018, 57, 10616−10624

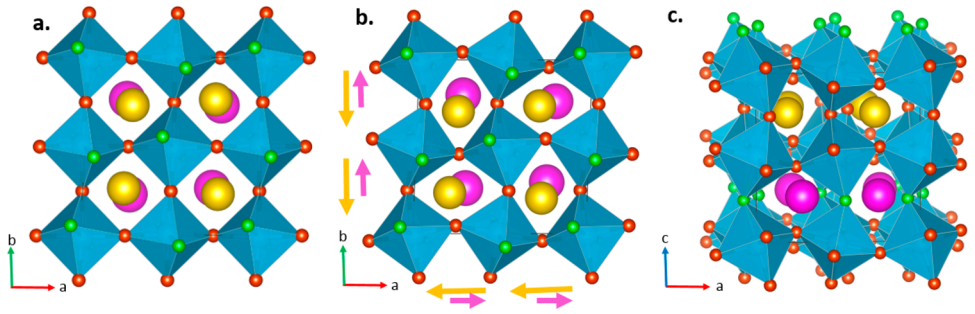

Figure 1. Crystal structures of $YCaFe_2O_5F$ with various tilt patterns. (a) Centrosymmetric phase having *Pmma* symmetry with $a^-a^-c^0$ tilts. (b) A polar phase with $Pmc2_1$ symmetry is obtained from (a) by adding in-phase octahedral rotations about the *c*-axis (c^+), coupled with noncompensating displacements of *A*-site cations, Y (yellow) and Ca (pink) here, in alternate layers. As indicated by arrows, Y atoms displace toward the left or bottom of the figure, while Ca atoms displace toward the right or top. (c) Structure of the polar phase as viewed along the *b*-axis, showing the antiphase a^-a^-tilts. We find that the polar phase is most stable with F (green) in the layer of Ca^{2+} cations. Oxygen atoms are shown in red, and FeO_5F octahedra are shown in blue color.

In this article, we report results from first-principles density functional theory (DFT) calculations showing anion substitution as a means to create Fe-based multiferroics with strong polarization and robust magnetic ordering above room temperature. Specifically, we propose that low-temperature fluorination of an oxygen-deficient double perovskite can be used to create multiferroics with a stoichiometry of $AA'Fe_2O_5F$, where the *A* and *A*′ cations are ordered into alternate layers—that can be obtained using layer-by-layer growth techniques. Fluorination of the oxygen-vacancy-ordered perovskites completes the corner connectivity of the octahedral network along all three dimensions, allowing hybrid improper ferroelectricity to operate. We describe the resulting multiferroics using DFT calculations and find that their calculated polarization can be as high as 13 $\mu C/cm^2$. For $YCaFe_2O_5F$, which prefers a polar configuration, we have calculated the magnetic exchange interactions and find that they are comparable to those in $YBaFe_2O_5$ and $YFeO_3$, both of which are magnetically ordered well above room temperature.[30,31] We have calculated the decomposition enthalpies of several of these fluorinated multiferroics, and we find that some of them are near or below the convex hull of competing compositions, indicating that they are either thermodynamically stable or metastable and it should be possible to synthesize them. This general approach of anion engineering in perovskites opens up new possibilities for creating room-temperature multiferroics.

COMPUTATIONAL DETAILS

We studied $AA'Fe_2O_5F$ perovskites using the plane wave DFT code Vienna Ab Initio Simulation Package (VASP)[32] version 5.4 with the projector augmented wave (PAW) method.[33,34] We used a 2 × 2 × 2 supercell of the 5-atoms ABX_3 perovskite unit cell to account for ion ordering and octahedral tilts. We used a 4 × 4 × 4 *k*-points grid for structural relaxations and a 10 × 10 × 10 grid for calculating the energy and electronic structure of the relaxed structures. An electronic convergence criterion (EDIFF) of 1×10^{-6} eV and a force convergence criterion (EDIFFG) of <0.01 eV/Å were used; certain calculations such as phonon calculations used a stricter force convergence criterion. We used a plane wave cutoff energy of 500 eV.

We used the PBEsol exchange−correlation functional,[35] which has been found to be optimal for perovskite oxyfluorides.[36] Additionally, to describe the strong correlations arising from the localized d-electrons of Fe, we used a Hubbard *U* parameter of 4 eV using the method of Dudarev et al.[37] In agreement with a previous work,[38] we found that this value accurately reproduced the charge and magnetic ordering of a possible unfluorinated starting compound, $YBaFe_2O_5$.[30] *G*-type antiferromagnetism, in which each Fe has a spin opposite to all its nearest neighbors, was imposed on each system unless stated otherwise. We also imposed layered ordering of the *A*, *A*′ cations along the *c*-axis in all the compounds investigated in this work. We used the SPuDS software[8] to generate starting structures with different octahedral tilt patterns and analyzed the distortion modes of optimized structures with ISODISTORT[39] as well as the Bilbao Crystallographic Server's PSEUDO and AMPLIMODES programs.[40,41] All tilted structures are described using Glazer's notation.[6] To find the likely ground states of this perovskite family, we studied $YBaFe_2O_5F$ and $LaCaFe_2O_5F$ because they represent two extremes of the size difference at the *A*-site. For these two systems, we relaxed them in many different combinations of octahedral tilt patterns and O/F anion orderings to find the ground state. The polar state with its preferred anion ordering is shown in Figure 1; the calculated energies of competing structures are available as Supporting Information. To reduce the computational cost, the remaining 10 systems with *A*-site pairs, LaBa, YBa, LaSr, LuSr, YSr, EuCa, YCa, YbCa, LuCa, and InCa, were only relaxed in the few most stable configurations observed in the two prototypes. We then used $YCaFe_2O_5F$ as a model system for the calculation of ferroelectric and magnetic properties because it has a stable polar ground state.

RESULTS AND DISCUSSION

We begin by briefly discussing the effect of fluorination of $YCaFeO_5$ on its electronic structure. Although $YCaFe_2O_5$ has not been synthesized, we can model it as a mixed-valence Fe^{2+}/Fe^{3+} structure with ordered oxygen vacancies in the Y layer, which has been observed for many $REBaM_2O_{6-x}$ (where *RE* is a rare-earth cation) compounds such as $YBaFe_2O_5$ and $YBaMn_2O_5$.[30,42−44] There are several possible combinations of magnetic and charge ordering; here, we have chosen to impose the $YBaFe_2O_5$ type. The low-temperature phase of $YBaFe_2O_5$ shows *G*-type antiferromagnetism, with "stripe" charge and orbital ordering along the *b*-axis. If $YCaFe_2O_5$ were to adopt a different charge ordering, it would not significantly affect the conclusions of this study, which is focused on the

DOI: 10.1021/acs.inorgchem.8b01253
Inorg. Chem. 2018, 57, 10616−10624

fluorinated $AA'FeO_5F$ perovskites. Fluorination of $YCaFe_2O_5$ is an oxidative process if the fluorine does not replace any of the oxygen, so the Fe^{2+}cations with d^6 configuration are oxidized to the Fe^{3+} state with d^5 configuration. We observe this effect in the density of states (DOS) shown in Figure 2,

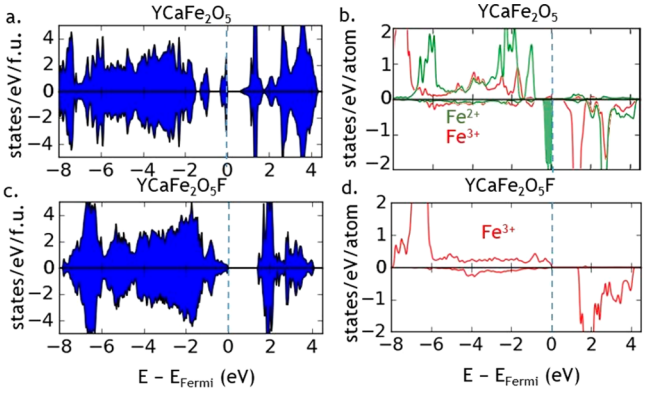

Figure 2. Electronic structure of $YCaFe_2O_5$ and $YCaFe_2O_5F$. (a) The electronic DOS of unfluorinated $YCaFe_2O_5$. (b) DOS projected onto the Fe d-states for both Fe^{2+} and Fe^{3+} oxidation states in $YCaFe_2O_5$. We only show the DOS of atoms that have a positive magnetic moment, but there are an equal number of atoms with negative moment. (c and d) The same data for the ground state of $YCaFe_2O_5F$ with Ca-layer fluorination in the $a^-a^-c^+$ tilt pattern. Fluorination leads to oxidation of Fe^{2+} ions to Fe^{3+}.

where the occupied Fe^{2+} d-states present near the Fermi level in $YCaFe_2O_5$ (the solid filled states in Figure 2b) are absent in the fluorinated compound (Figure 2d). We also observe that fluorination of $YCaFe_2O_5$ increases the band gap.

We will now examine the magnetic properties of $YCaFeO_5F$ and its likelihood of remaining magnetically ordered at room temperature. Based on the Goodenough−Kanamori rules for superexchange,[45,46] this compound is expected to be an antiferromagnet due to the presence of antiferromagnetic interactions between neighboring Fe^{3+} cations. Our calculations confirm that *G*-type antiferromagnetism is more stable than *A*- and *C*-type antiferromagnetism as well as the ferromagnetic state. The calculated magnetic moments on Fe^{3+} are 4.0−4.1 μ_B, less than the theoretical value of 5 μ_B, but it is important to note that the calculated value comes from integration across a somewhat arbitrary atomic sphere, while the theoretical value assumes that Fe^{3+} has exactly 5 d-electrons which corresponds to purely ionic bonding.[47] We also find that the O/F anions carry small magnetic moments due to covalent interactions. To estimate the Néel temperature (T_N) for transition from antiferromagnetic to paramagnetic ordering, it is necessary to determine the strength of the individual superexchange interactions acting through the Fe−O−Fe or Fe−F−Fe bond pathways. We considered magnetic interactions up to the third nearest neighbors and extracted the interactions J_1−J_9 by fitting a Heisenberg model to the total energy of 10 different magnetic configurations that were chosen randomly, subject to the constraint that the resulting set of equations were linearly independent. The Hamiltonian is given by

$$H = E_0 - \sum_{i \neq j} J_{ij} S_i S_j \tag{1}$$

where $S = 5/2$ is the theoretical spin of the Fe^{3+} ion. The exchange constants are dependent on the choice between theoretical or calculated magnetic moments, but the magnetic energy per atom and therefore the transition temperature do not depend on this choice because the moment cancels when summing up the interactions for each atom. We found the exchange constants for $YCaFe_2O_5F$ with the ground state $a^-a^-c^+$ tilting and Ca-layer fluorination. We made the approximation that structure is the same along *a* and *b* directions, since it has a = 7.635 Å and b = 7.607 Å, but we considered two different types of in-plane nearest-neighbor interactions, J_3 and J_4, as shown in Figure 3. There are two

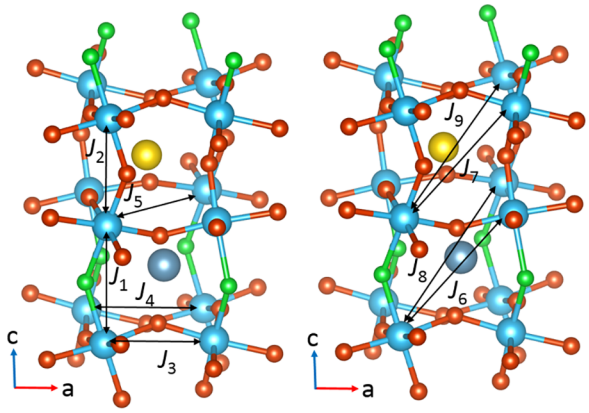

E_0/f.u.	J_1	J_2	J_3	J_4
-75.10 eV	-1.4 meV	-8.4 meV	-9.4 meV	-5.9 meV
J_5	J_6	J_7	J_8	J_9
-0.43 meV	0.16 meV	-0.07 meV	-0.27 meV	-0.38 meV

Figure 3. Magnetic exchange constants between Fe^{3+} ions in $YCaFe_2O_5F$. A positive sign indicates a ferromagnetic interaction. The atomic model on the left shows the nearest-neighbor interactions, which are stronger than the second and third nearest-neighbor interactions shown on the right. The size of the *A*-site cations has been reduced for clarity.

types of in-plane bonds due to the broken mirror symmetry from cation ordering: interaction J_3 with an Fe−Fe distance of 3.71 Å and an Fe−O−F bond angle of 143°; and J_4 with an Fe−Fe distance of 3.93 Å and a bond angle of 151°.

Based on the calculated strengths of various exchange interactions, as shown in Figure 3, we find that the nearest-neighbor interactions J_1−J_4 are dominant, with strong antiferromagnetism leading to the *G*-type AFM ground state. The total magnetic stabilization of each Fe ion with respect to the magnetically disordered state is given by[38]

$$\frac{1}{2}\sum_i J_i z_i \left(\frac{5}{2}\right)^2 = -136\text{meV} \tag{2}$$

where z_i is the number of interactions of each type that the ion has. If only the nearest-neighbor interactions J_1−J_4 are taken into account, this value becomes −125 meV/Fe. While T_N could in principle be calculated from the exchange constants using a mean-field approximation or with Monte Carlo simulations, in practice this may give inaccurate results due to the empirical nature of the Hubbard U parameter.[48,49] Instead we have compared the magnetic stabilization for $YCaFe_2O_5F$ with those calculated using the same DFT

DOI: 10.1021/acs.inorgchem.8b01253
Inorg. Chem. 2018, 57, 10616−10624

parameters for related compounds whose T_N are known experimentally. For $YFeO_3$, with T_N = 655 K,[31] we calculate an energy stabilization in *G*-type AFM of −106 meV/Fe, including only nearest-neighbor interactions. For $YBaFe_2O_5$, with a slightly different structure and T_N = 410 K,[30] the calculated stabilization of *G*-type AFM is −115 meV/Fe including up to second-nearest-neighbor interactions, which is similar to a previous report.[38] Therefore, we expect that the strong exchange interactions in $YCaFe_2O_5F$ will lead to a robust magnetic ordering with a Neél temperature at least as high as 410 K.

We note that the Fe−F−Fe exchange constant J_1 is only −1.4 meV, much smaller than the Fe−O−Fe interactions J_2−J_4. The reason for this is the decreased covalency of the bond through F, which has much lower valence orbital energies than O. Goodenough[45] observed that superexchange becomes weaker when more energy is required to excite an electron from the filled anion p-orbital to the half-empty cation d-orbital. This effect can be seen in the site-projected DOS of $YCaFe_2O_5F$, shown in Supporting Information. Weakened superexchange is frequently observed in distorted perovskite oxides when octahedral tilting decreases the orbital overlap,[50] but replacing O with F has an even greater effect, as shown in several experiments.[51−54] For instance, pseudocubic $AgFeOF_2$ with very little tilting has a Neél temperature of 480 K,[52] much lower than that of the tilted perovskites $SrFeO_2F$ (T_N = 710 K)[55] or $LaFeO_3$ (T_N = 740 K),[56] which might be expected to have weaker superexchange due to their tilts. In another experiment, fluorination of La_2NiO_{4+d} to $La_2NiO_3F_2$ reduced the Neél temperature from 330 to 49 K, despite the fact that the oxidation state of Ni remained the same.[53] The dominant factor is clearly the reduced covalency of the Fe−F−Fe bond pathway. In the case of $AA'Fe_2O_5F$, the total superexchange remains relatively strong because only one O out of six is replaced.

If the anion sublattice is completely ordered, it could affect the magnetic ordering pattern and Neél temperature as well. Although $YCaFe_2O_5F$ is predicted to retain *G*-type antiferromagnetism, the J_1 interaction across the fluorinated +2 layer may become ferromagnetic in related compounds with even more octahedral tilting, leading to a magnetic state with a doubled unit cell along the *c*-axis. However, none of the cation pairs in this study have octahedral tilting more than 2° stronger than YCa. Furthermore, as we have shown in the Supporting Information, entropy may stabilize an anion-disordered state as seen in many other oxyfluorides.[57,58] In this case, a three-dimensional network of Fe−O−Fe bonds is expected to retain the strong *G*-type antiferromagnetism. The magnitude of the electric polarization is unlikely to be affected by anion disorder.

We have just seen the advantage of using the d^5 Fe^{3+} at the *B*-site to optimize the magnetic properties. In an antiferromagnet, a high Néel temperature requires strong superexchange interactions between the *B*-site cations, operating through the *B*−*X*−*B* bonds. Fe^{3+} meets this criterion very well,[59,60] with $LaFeO_3$ showing an antiferromagnetic Néel temperature of 750 K compared to 100 K for $LaMnO_3$ or 320 K for $LaCrO_3$.[61] For this reason, $AA'Fe_2O_6$ is a promising family of potential multiferroics, while multiferroics with other *B*-site cations rarely have room-temperature magnetic ordering. However, this robust magnetism comes at a price. Charge balance in an Fe^{3+} double perovskite oxide requires that the oxidation states of the two *A*-site cations sum to +6, and since small +4 cations rarely occupy the *A*-site, in practice these hybrid improper ferroelectrics must have two +3 *A*-site cations such as lanthanides.[48,62,63] The net polarization in this case results only from the size difference between the two lanthanides, and the two ionic displacements cancel to a large extent. It would be preferable to use a larger +2 cation at one of the *A* sites to maximize the polarization[64] and improve the precision of cation layer ordering.[62] But if the total cation charge is altered in this way, charge balance then leads to oxygen-deficient structures to avoid the formation of the less favorable Fe^{4+} oxidation state.[65−69] Furthermore, the oxygen vacancies in such perovskites are often observed to undergo ordering along specific planes, which results in the breaking of the cooperative octahedral tilt pattern necessary for the hybrid improper ferroelectric mechanism, although anion-deficient structures can still be polar under some circumstances.[69,70] Substitution of fluoride with −1 charge, compared to oxide's −2, lifts this constraint and permits the *A*-site charge to take values other than +3. Therefore, fluorination of vacancy-ordered perovskites offers the chance to optimize the ferroelectricity with only a small effect on the magnetism, as long as there is still more oxide than fluoride.

To confirm if $YCaFe_2O_5F$ is a hybrid improper ferroelectric, we have calculated the polarization of its ground-state phase with F atoms in the Ca layer, having a $Pmc2_1$ space group and $a^-a^-c^+$ tilts, using the Berry-phase method.[71,72] The calculated polarization values were mapped to a single polarization branch using the Pymatgen software package.[73] We find that $YCaFe_2O_5F$ has a spontaneous polarization of 10.3 $\mu C/cm^2$. The expected switching mode is a reversal of the c^+ tilt, moving through a *Pmma* centrosymmetric phase with a calculated energy barrier of 64 meV/f.u. The switching barrier of a useful ferroelectric should be large enough to be stable against thermal fluctuations, but low enough that a reasonable coercive field can overcome it. It is not possible to calculate the ferroelectric/paraelectric transition temperature or required coercive field directly from the height of the theoretical switching barrier, since the actual switching mechanism may involve domain wall motion rather than a concerted motion of all the atoms as we have calculated here.[74] However, the calculated barrier of 64 meV/f.u. is exactly the same as that of the Ruddlesden−Popper phase $Ca_3Ti_2O_7$,[74] which has a different switching mechanism but is known to be experimentally switchable.[20]

To investigate the presence of any magnetoelectric coupling, we have calculated the exchange interactions along the distortion mode that switches the polarization. We find that switching the polarization also affects the magnetic exchange constants, since the switching pathway temporarily eliminates the c^+ octahedral rotations. This improves the overlap of Fe d-states with the p-states of O/F and increases the strength of the superexchange interactions. As we have established that longer-ranged interactions are relatively unimportant in this system, for clarity, we have used a simplified Heisenberg model with only a single nearest-neighbor interaction (J_{NN}), as shown in Figure 4. We find that the centrosymmetric *Pmma* phase shows increased superexchange between nearest neighbors with the average nearest-neighbor exchange constant being −8.18 meV compared to −7.17 eV in the ground state. The ground-state $Pmc2_1$ phase is also expected to show a linear magnetoelectric coupling through the Dzyaloshinskii−Moriya effect because there is no inversion center between the neighboring iron atoms.[48] Therefore, the magnetic moments are expected to be canted and to respond to the switching mode. However,

DOI: 10.1021/acs.inorgchem.8b01253
Inorg. Chem. 2018, 57, 10616−10624

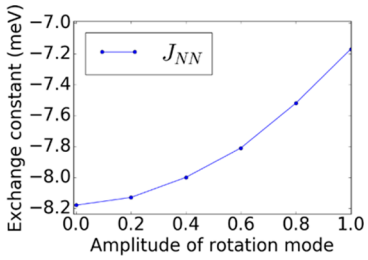

Figure 4. Variation of the nearest-neighbor (NN) exchange constant J_{NN} with the amplitude of the polarity-switching mode, which combines opposite polar displacements of successive *A*-site layers and the reversal of the c^+ octahedral tilt.

quantifying the strength of this coupling would require expensive noncollinear magnetism calculations, which are outside the scope of this article.

The polarization predicted (10.3 μC/cm^2) for $YCaFe_2O_5F$ is not unusually large. For comparison, $LuLaFe_2O_6$ with exclusively +3 cations at the *A*-site was predicted to have a polarization of 11.6 μC/cm^2.[48] While the introduction of the Ca^{2+} tends to reduce the cancellation of the opposing *A*-site displacements, the size difference between Y^{3+} and Ca^{2+} is only 0.1 Å according to their 8-coordinate Shannon radii.[75] Hence, in the following, we have investigated the possibility to achieve higher polarization by changing the size ratio of the two *A*-site cations, but keeping their charge ratio fixed at +2/+3.

The substitution of different cations at the *A*-site is expected to have a strong influence on the octahedral tilt pattern, since the main purpose of these tilts is to optimize the coordination environment of the *A*-site cation.[76] Specifically, a smaller *A*-site cation causes increased tilting and tends to favor the $a^-a^-c^+$ tilt pattern, which mitigates the anion−anion repulsion around the small cation.[76] We considered Ba, Sr, and Ca for the 2+ cation and chose the 3+ cation from La, Y, Eu, Lu, Yb, and In. For each pair of *A*-site cations, we show the calculated polarization in Figure 5. Compounds having the polar phase ($a^-a^-c^+$, $Pmc2_1$) as the ground state are shown in blue and those having a nonpolar phase, such as $a^0b^-c^-$, as the ground state are shown in red. We find that compounds having small 2+ cations, such as Ca, are more likely to prefer the polar phase, which is consistent with the expectation that small *A*-site cations favor $a^-a^-c^+$tilt pattern. However, other factors such as size difference also play a role. CaIn and SrLu have average *A*-site cations sizes less than or equal to those of stable polar compounds, but their calculated ground state has a $a^0b^-c^-$ tilt pattern and fluorine in the Fe layers of the compound. Two of the compounds, EuCa and LaCa, are listed as having zero polarization even though they are both noncentrosymmetric. In these compounds, the small ionic polarization is screened almost completely by an opposing electronic polarization.

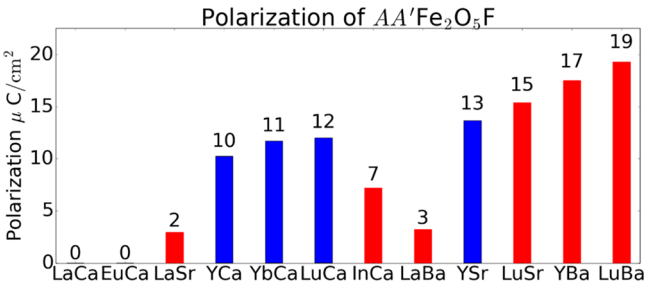

Figure 5. Calculated polarization of $AA'Fe_2O_5F$ double perovskites with varying size difference of the *A* and *A*′ cations. The polarization has been calculated in the polar $Pmc2_1$ space group with $a^-a^-c^+$ tilt and F in the layer of the +2 cations. Blue bars indicate that the system prefers this polar phase, while red bars indicate that there is a competing nonpolar phase that is more stable.

We find that the polarization generally increases with increasing size difference, as predicted by previous first-principles calculations on oxide hybrid improper ferroelectrics.[64,77] The authors of these studies proposed that effective hybrid improper ferroelectrics should have large *A*-site cations and large size differences between the *A*-site cations, in order to maximize polarization while minimizing the ferroelectric switching barrier, estimated as the energy difference between the $a^-a^-c^+$ tilt pattern and the centrosymmetric $a^-a^-c^0$ pattern. However, in the oxyfluoride perovskites studied here, attempting to lower the switching barrier by destabilizing the c^+ distortion mode with large cations leads to a nonpolar ground state with a completely different tilt pattern, $a^0b^-c^-$ in the $C2/m$ space group. This is likely to limit the polarization that can be achieved experimentally. Our results also highlight the need for further investigation of whether the same effect occurs in pure oxide perovskites. We note that it may be possible to use epitaxial strain to stabilize the polar phase of high-polarization compounds such as $LuBaFe_2O_5F$, since octahedral tilting is strongly coupled to strain.[78]

Finally, we have considered whether it is likely that these fluorinated multiferroics can be synthesized. The data in Figure 5 indicate that a small *A*-site size difference is required to achieve the $a^-a^-c^+$ tilt pattern. However, this small size difference when combined with the small charge difference of +2 and +3 cations makes it unlikely that the compounds will spontaneously order into alternating layers at the *A*-site, as required by the hybrid improper mechanism. To test this possibility, we have calculated the energy of a cation-disordered special quasirandom structure (SQS)[79,80] of $YCaFeO_6$ in the $a^-b^+c^-$ tilt pattern, which the untilted structure spontaneously adopted during relaxation. We find that the ordered and disordered structures have the same energy to within 1 meV/f.u., with entropy likely to produce disorder at experimental temperatures. Therefore, we expect that it will be necessary to use layer-by-layer growth techniques to impose layered *A*-site cation ordering artificially. The exact oxygen stoichiometry of these artificially ordered perovskite oxides is expected to depend on the reduction conditions.[81] They may have the $YBaFe_2O_5$ vacancy-ordered structure with Fe^{3+}/Fe^{2+} charge ordering, as modeled in this work, or a brownmillerite structure with charge ordering,[66] or they may adopt an $AA'Fe_2O_{5.5}$ stoichiometry to achieve a uniform Fe^{3+} state.[9,82]

We have also considered the possibility of decomposition to competing binary and ternary phases. Similar oxyfluoride perovskites are often metastable,[21] due to the high stability of the binary fluorides which would result from decomposition. We can calculate the stability of a compound by comparing its energy with respect to its most stable reactants or products. Compounds that cannot decompose into more stable products lie on the convex hull of the phase diagram, while those that can are above the hull. Previous data mining of the calculated formation energies of known compounds has shown that the 90th percentile of metastable compounds are 67 meV/atom above the convex hull.[83] Hence, we can use a formation energy of <70 meV/atom as a criterion to evaluate metastable

DOI: 10.1021/acs.inorgchem.8b01253
Inorg. Chem. 2018, 57, 10616−10624

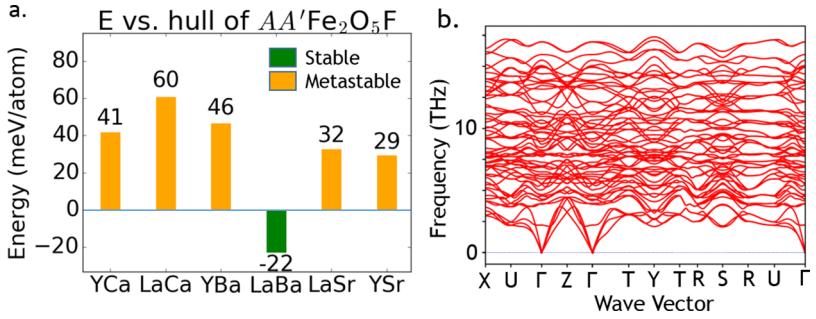

Figure 6. Thermodynamic and dynamic stability of polar $AA'Fe_2O_5F$ multiferroics. (a) The calculated formation energies of six representative compounds, including YCa. A negative energy corresponds to a stable compound that lies on the convex hull. (b) Phonon band structure of the polar ground state of $YCaFe_2O_5F$, which has no soft phonon modes and is therefore dynamically stable.

compounds that can be synthesized. We have used the Open Quantum Materials Database[84] to identify the most favorable decomposition pathway for six of our compounds, then calculated the formation energy relative to the convex hull. For this calculation, we found the energy of the decomposition products using the same DFT settings we previously used for the oxyfluorides. As an example, $YCaFe_2O_5F$ is most susceptible to decompose by the reaction

$$YCaFe_2O_5F \rightarrow YFeO_3 + 0.5(CaFe_2O_4) + 0.5(CaF_2)$$

and the change in energy of this process is −41.7 meV/atom, placing $YCaFe_2O_5F$ 41.7 meV/atom above the convex hull but within the region where metastable compounds are plausible. The formation energies vs the convex hull of six representative compounds are shown in Figure 6a.

Synthesis of metastable compounds usually occurs when the compound is kinetically trapped and cannot transform to more stable phases. In perovskites, cations are not mobile at low temperatures, but anions are, which is the basis for the "soft chemistry" topochemical techniques which modify the anion sublattice of a stable oxide but leave the rest of the structure unchanged.[21,85,86] Because the cations are not mobile, they cannot phase segregate to low-energy binary or ternary compounds once fluorine is added.[87] To study this kinetic trapping, we have calculated the phonon band structure of the polar phase of $YCaFe_2O_5F$. We do not observe any soft modes as shown in Figure 6b, indicating that the structure is dynamically stable with respect to small displacements of its atoms. It is interesting to note that $LaSrFe_2O_5F$, which we predict to be metastable based on the formation energy (32 meV/atom), has been synthesized with cation disorder at the *A*-site using low-temperature fluorination.[88] Centrosymmetric $La_{2-x}Sr_xFe_2O_{6-x}F_x$ was obtained across the wide composition range $x = 0$ to $x = 2$, using fluorine like a codopant to maintain charge balance.[88,89] As expected, the compound was metastable but could be made as a single phase at relatively a low temperature (400 °C). Therefore, we expect that similar low-temperature fluorination techniques combined with layered *A*-site ordering can be used to produce many of the compounds considered here.

CONCLUSIONS

In summary, we have used DFT calculations to investigate the addition of fluorine to layer-ordered double perovskites with Fe at the *B*-site, with the goal of developing new hybrid improper ferroelectrics with high magnetic ordering temperature. We find that using a +2 and a +3 cation at the *A*-site can increase the polarization of the polar phase with $a^-a^-c^+$ tilts to as high as 19.3 $\mu C/cm^2$. However, not all of the possible combinations of *A*-site cations are expected to lead to a polar ground state, since the $a^0b^-c^-$ tilt pattern becomes increasingly competitive as the average size and size difference of the *A*-site cations increase. The compounds with a predicted polar ground state tend to have less polarization and would require layer-by-layer growth techniques, such as molecular beam epitaxy, to impose cation ordering. The fluorinated perovskites are expected to have high magnetic ordering temperatures due to the strong superexchange interactions between Fe^{3+} ions, and our calculations show that one example, $YCaFe_2O_5F$, has superexchange interactions at least as strong as those of $YFeO_3$ and $YBaFe_2O_5$, which both order above 400 K. By symmetry, these $Pmc2_1$ multiferroics should also show linear magnetoelectric coupling when the polarization is switched.

Based on these results, we expect that low-temperature fluorination combined with layered ordering of cations will be a valuable tool for synthetic researchers attempting to create new multiferroics. The main advantage of hybrid improper ferroelectrics for this purpose is that the ferroelectricity is generated at the *A*-site, while the magnetism is generated at the *B*-site, which avoids the incompatibility between the two types of ordering which would otherwise make multiferroics rare.[12] However, the two cation states are still linked by the requirement that the sum of their charges equal +6 per ABX_3 cell to avoid anion deficiency. The use of anion engineering to balance charge loosens this constraint and can most likely be applied to other related systems, such as manganites, cobaltites, nickelates, and cuprate perovksites.

ASSOCIATED CONTENT

Supporting Information

The Supporting Information is available free of charge on the ACS Publications website at DOI: 10.1021/acs.inorgchem.8b01253.

Data tables showing stability of different phases and VESTA images of anion orderings (PDF)

AUTHOR INFORMATION

Corresponding Authors

*E-mail: steven.t.hartman@wustl.edu.
*E-mail: rmishra@wustl.edu.

ORCID

Rohan Mishra: 0000-0003-1261-0087

Notes

The authors declare no competing financial interest.

DOI: 10.1021/acs.inorgchem.8b01253
Inorg. Chem. 2018, 57, 10616−10624

■ ACKNOWLEDGMENTS

This work was partially supported by National Science Foundation (NSF) grants CBET-1729787 and DMR-1806147 and the Consortium for Clean Coal Utilization (CCCU) at Washington University. This work used computational resources of the eXtreme Science and Engineering Discovery Environment (XSEDE), which is supported by the NSF ACI-1053575.

■ REFERENCES

(1) Cava, R. J.; Batlogg, B.; Krajewski, J. J.; Farrow, R.; Rupp, L. W.; White, A. E.; Short, K.; Peck, W. F.; Kometani, T. Superconductivity near 30-K without Copper - the $Ba_{0.6}K_{0.4}BiO_3$Perovskite. *Nature* **1988**, *332* (6167), 814−816.

(2) Kobayashi, K. I.; Kimura, T.; Sawada, H.; Terakura, K.; Tokura, Y. Room-temperature magnetoresistance in an oxide material with an ordered double-perovskite structure. *Nature* **1998**, *395* (6703), 677−680.

(3) Mishra, R.; Restrepo, O. D.; Woodward, P. M.; Windl, W. First-Principles Study of Defective and Nonstoichiometric Sr_2FeMoO_6. *Chem. Mater.* **2010**, *22* (22), 6092−6102.

(4) Jang, J. H.; Kim, Y. M.; He, Q.; Mishra, R.; Qiao, L.; Biegalski, M. D.; Lupini, A. R.; Pantelides, S. T.; Pennycook, S. J.; Kalinin, S. V.; Borisevich, A. Y. In Situ Observation of Oxygen Vacancy Dynamics and Ordering in the Epitaxial $LaCoO_3$System. *ACS Nano* **2017**, *11* (7), 6942−6949.

(5) Jeen, H.; Choi, W. S.; Biegalski, M. D.; Folkman, C. M.; Tung, I. C.; Fong, D. D.; Freeland, J. W.; Shin, D.; Ohta, H.; Chisholm, M. F.; Lee, H. N. Reversible redox reactions in an epitaxially stabilized $SrCoO_{(x)}$oxygen sponge. *Nat. Mater.* **2013**, *12* (11), 1057−63.

(6) Glazer, A. The classification of tilted octahedra in perovskites. *Acta Crystallogr., Sect. B: Struct. Crystallogr. Cryst. Chem.* **1972**, *28* (11), 3384−3392.

(7) Woodward, P. M. Octahedral Tilting in Perovskites. I. Geometrical Considerations. *Acta Crystallogr., Sect. B: Struct. Sci.* **1997**, *53* (1), 32−43.

(8) Lufaso, M. W.; Woodward, P. M. Prediction of the crystal structures of perovskites using the software program SPuDS. *Acta Crystallogr., Sect. B: Struct. Sci.* **2001**, *57*, 725−738.

(9) King, G.; Woodward, P. M. Cation ordering in perovskites. *J. Mater. Chem.* **2010**, *20* (28), 5785−5796.

(10) Anderson, M. T.; Greenwood, K. B.; Taylor, G. A.; Poeppelmeier, K. R. B-Cation Arrangements in Double Perovskites. *Prog. Solid State Chem.* **1993**, *22* (3), 197−233.

(11) Schlom, D. G.; Chen, L.-Q.; Pan, X.; Schmehl, A.; Zurbuchen, M. A. A Thin Film Approach to Engineering Functionality into Oxides. *J. Am. Ceram. Soc.* **2008**, *91* (8), 2429−2454.

(12) Hill, N. A. Why Are There so Few Magnetic Ferroelectrics? *J. Phys. Chem. B* **2000**, *104* (29), 6694−6709.

(13) Lee, J. H.; Fang, L.; Vlahos, E.; Ke, X.; Jung, Y. W.; Kourkoutis, L. F.; Kim, J. W.; Ryan, P. J.; Heeg, T.; Roeckerath, M.; Goian, V.; Bernhagen, M.; Uecker, R.; Hammel, P. C.; Rabe, K. M.; Kamba, S.; Schubert, J.; Freeland, J. W.; Muller, D. A.; Fennie, C. J.; Schiffer, P.; Gopalan, V.; Johnston-Halperin, E.; Schlom, D. G. A strong ferroelectric ferromagnet created by means of spin-lattice coupling. *Nature* **2010**, *466* (7309), 954−8.

(14) Seshadri, R.; Hill, N. A. Visualizing the Role of Bi 6s "Lone Pairs" in the Off-Center Distortion in Ferromagnetic $BiMnO_3$. *Chem. Mater.* **2001**, *13* (9), 2892−2899.

(15) Young, J.; Lalkiya, P.; Rondinelli, J. M. Design of non-centrosymmetric perovskites from centric and acentric basic building units. *J. Mater. Chem. C* **2016**, *4* (18), 4016−4027.

(16) Benedek, N. A.; Fennie, C. J. Hybrid Improper Ferroelectricity: A Mechanism for Controllable Polarization-Magnetization Coupling. *Phys. Rev. Lett.* **2011**, *106* (10), 107204.

(17) Bousquet, E.; Dawber, M.; Stucki, N.; Lichtensteiger, C.; Hermet, P.; Gariglio, S.; Triscone, J. M.; Ghosez, P. Improper ferroelectricity in perovskite oxide artificial superlattices. *Nature* **2008**, *452* (7188), 732−6.

(18) Rondinelli, J. M.; Fennie, C. J. Octahedral rotation-induced ferroelectricity in cation ordered perovskites. *Adv. Mater.* **2012**, *24* (15), 1961−8.

(19) Zuo, P.; Colin, C. V.; Klein, H.; Bordet, P.; Suard, E.; Elkaim, E.; Darie, C. Structural Study of a Doubly Ordered Perovskite Family $NaLnCoWO_6$(Ln = Y, La, Pr, Nd, Sm, Eu, Gd, Tb, Dy, Ho, Er, Yb): Hybrid Improper Ferroelectricity in Nine New Members. *Inorg. Chem.* **2017**, *56* (14), 8478−8489.

(20) Oh, Y. S.; Luo, X.; Huang, F.-T.; Wang, Y.; Cheong, S.-W. Experimental demonstration of hybrid improper ferroelectricity and the presence of abundant charged walls in $(Ca,Sr)_3Ti_2O_7$crystals. *Nat. Mater.* **2015**, *14* (4), 407−413.

(21) Clemens, O.; Slater, P. R. Topochemical modifications of mixed metal oxide compounds by low-temperature fluorination routes. *Rev. Inorg. Chem.* **2013**, *33*, 105.

(22) Kobayashi, Y.; Tsujimoto, Y.; Kageyama, H. Property Engineering in Perovskites via Modification of Anion Chemistry. *Annu. Rev. Mater. Res.* **2018**, *48* (1), 303.

(23) Kageyama, H.; Hayashi, K.; Maeda, K.; Attfield, J. P.; Hiroi, Z.; Rondinelli, J. M.; Poeppelmeier, K. R. Expanding frontiers in materials chemistry and physics with multiple anions. *Nat. Commun.* **2018**, *9*, 772.

(24) Moon, E. J.; Xie, Y.; Laird, E. D.; Keavney, D. J.; Li, C. Y.; May, S. J. Fluorination of Epitaxial Oxides: Synthesis of Perovskite Oxyfluoride Thin Films. *J. Am. Chem. Soc.* **2014**, *136* (6), 2224−2227.

(25) Onozuka, T.; Chikamatsu, A.; Katayama, T.; Hirose, Y.; Harayama, I.; Sekiba, D.; Ikenaga, E.; Minohara, M.; Kumigashira, H.; Hasegawa, T. Reversible Changes in Resistance of Perovskite Nickelate $NdNiO_3$Thin Films Induced by Fluorine Substitution. *ACS Appl. Mater. Interfaces* **2017**, *9* (12), 10882−10887.

(26) Altintas, S. P.; Mahamdioua, N.; Amira, A.; Terzioglu, C. Effect of anionic substitution on the structural and magneto-electrical properties of La-Ca-Mn-O perovskite manganites. *J. Magn. Magn. Mater.* **2014**, *368* (Supplement C), 111−115.

(27) Moon, K. H.; Avdeev, M.; Kim, Y.-I. Crystal structure and optical property of complex perovskite oxynitrides $ALi_{0.2}Nb_{0.8}O_{2.8}N_{0.2}ANa_{0.2}Nb_{0.8}O_{2.8}N_{0.2}$and $AMg_{0.2}Nb_{0.8}O_{2.6}N_{0.4}$(A = Sr, Ba). *J. Solid State Chem.* **2017**, *254*, 1−8.

(28) Oka, D.; Hirose, Y.; Kamisaka, H.; Fukumura, T.; Sasa, K.; Ishii, S.; Matsuzaki, H.; Sato, Y.; Ikuhara, Y.; Hasegawa, T. Possible ferroelectricity in perovskite oxynitride $SrTaO_2N$ epitaxial thin films. *Sci. Rep.* **2015**, *4*, 4987.

(29) Kubo, A.; Giorgi, G.; Yamashita, K. Anion Ordering in $CaTaO_2N$: Structural Impact on the Photocatalytic Activity. Insights from First-Principles. *Chem. Mater.* **2017**, *29* (2), 539−545.

(30) Woodward, P. M.; Karen, P. Mixed valence in $YBaFe_2O_5$. *Inorg. Chem.* **2003**, *42* (4), 1121−9.

(31) Shang, M. Y.; Zhang, C. Y.; Zhang, T. S.; Yuan, L.; Ge, L.; Yuan, H. M.; Feng, S. H. The multiferroic perovskite $YFeO_3$. *Appl. Phys. Lett.* **2013**, *102* (6), 062903.

(32) Kresse, G.; Furthmüller, J. Efficient iterative schemes for ab initio total-energy calculations using a plane-wave basis set. *Phys. Rev. B: Condens. Matter Mater. Phys.* **1996**, *54* (16), 11169−11186.

(33) Kresse, G.; Joubert, D. From ultrasoft pseudopotentials to the projector augmented-wave method. *Phys. Rev. B: Condens. Matter Mater. Phys.* **1999**, *59* (3), 1758−1775.

(34) Blöchl, P. E. Projector augmented-wave method. *Phys. Rev. B: Condens. Matter Mater. Phys.* **1994**, *50* (24), 17953−17979.

(35) Perdew, J. P.; Ruzsinszky, A.; Csonka, G. I.; Vydrov, O. A.; Scuseria, G. E.; Constantin, L. A.; Zhou, X.; Burke, K. Restoring the Density-Gradient Expansion for Exchange in Solids and Surfaces. *Phys. Rev. Lett.* **2008**, *100* (13), 136406.

(36) Charles, N.; Rondinelli, J. M. Assessing exchange-correlation functional performance for structure and property predictions of oxyfluoride compounds from first principles. *Phys. Rev. B: Condens. Matter Mater. Phys.* **2016**, *94* (17), 174108.

DOI: 10.1021/acs.inorgchem.8b01253
Inorg. Chem. 2018, 57, 10616−10624

(37) Dudarev, S. L.; Botton, G. A.; Savrasov, S. Y.; Humphreys, C. J.; Sutton, A. P. Electron-energy-loss spectra and the structural stability of nickel oxide: An LSDA+U study. *Phys. Rev. B: Condens. Matter Mater. Phys.* **1998**, *57* (3), 1505−1509.
(38) Zhang, Y.; Whangbo, M.-H. Density Functional Analysis of the Spin Exchange Interactions and Charge Order Patterns in the Layered Magnetic Oxides $YBaM_2O_5$(M = Mn, Fe, Co). *Inorg. Chem.* **2011**, *50* (21), 10643−10647.
(39) Campbell, B. J.; Stokes, H. T.; Tanner, D. E.; Hatch, D. M. ISODISPLACE: a web-based tool for exploring structural distortions. *J. Appl. Crystallogr.* **2006**, *39* (4), 607−614.
(40) Capillas, C.; Tasci, E. S.; de la Flor, G.; Orobengoa, D.; Perez-Mato, J. M.; Aroyo, M. I. A new computer tool at the Bilbao Crystallographic Server to detect and characterize pseudosymmetry. *A. Kristallogr. - Cryst. Mater.* **2011**, *226*, 186.
(41) Orobengoa, D.; Capillas, C.; Aroyo, M. I.; Perez-Mato, J. M. AMPLIMODES: symmetry-mode analysis on the Bilbao Crystallographic Server. *J. Appl. Crystallogr.* **2009**, *42* (5), 820−833.
(42) Millange, F.; Suard, E.; Caignaert, V.; Raveau, B. $YBaMn_2O_5$Crystal and magnetic structure reinvestigation. *Mater. Res. Bull.* **1999**, *34* (1), 1−9.
(43) Karen, P.; Woodward, P. M. Synthesis and structural investigations of the double perovskites $REBaFe_2O_{5+w}$(RE = Nd, Sm). *J. Mater. Chem.* **1999**, *9* (3), 789−797.
(44) Woodward, P. M.; Suard, E.; Karen, P. Structural tuning of charge, orbital, and spin ordering in double-cell perovskite series between $NdBaFe_2O_5$and $HoBaFe_2O_5$. *J. Am. Chem. Soc.* **2003**, *125* (29), 8889−99.
(45) Goodenough, J. B. An interpretation of the magnetic properties of the perovskite-type mixed crystals $La_{1-x}Sr_xCoO_{3-\lambda}$. *J. Phys. Chem. Solids* **1958**, *6* (2−3), 287−297.
(46) Kanamori, J. Superexchange interaction and symmetry properties of electron orbitals. *J. Phys. Chem. Solids* **1959**, *10* (2−3), 87−98.
(47) Jansen, M.; Wedig, U. A Piece of the Picture—Misunderstanding of Chemical Concepts. *Angew. Chem., Int. Ed.* **2008**, *47* (52), 10026−10029.
(48) Ghosh, S.; Das, H.; Fennie, C. J. Linear magnetoelectricity at room temperature in perovskite superlattices by design. *Phys. Rev. B: Condens. Matter Mater. Phys.* **2015**, *92* (18), 184112.
(49) Santana, J. A.; Mishra, R.; Krogel, J. T.; Borisevich, A. Y.; Kent, P. R.C.; Pantelides, S. T.; Reboredo, F. A. Quantum Many-Body Effects in Defective Transition-Metal-Oxide Superlattices. *J. Chem. Theory Comput.* **2017**, *13* (11), 5604−5609.
(50) Marthinsen, A.; Faber, C.; Aschauer, U.; Spaldin, N. A.; Selbach, S. M. Coupling and competition between ferroelectricity, magnetism, strain, and oxygen vacancies in $AMnO_3$perovskites. *MRS Commun.* **2016**, *6* (3), 182−191.
(51) Bashkirov, S. S.; Liberman, A. B.; Manenkova, L. K.; Men, A. N.; Khasanov, A. M. Superexchange interactions and magnetic microstructures of oxyfluoride ferrospinels. *Sov. Phys. J.* **1984**, *27* (7), 580−582.
(52) Takeiri, F.; Yamamoto, T.; Hayashi, N.; Hosokawa, S.; Arai, K.; Kikkawa, J.; Ikeda, K.; Honda, T.; Otomo, T.; Tassel, C.; Kimoto, K.; Kageyama, H. $AgFeOF_2$: A Fluorine-Rich Perovskite Oxyfluoride. *Inorg. Chem.* **2018**, *57*, 6686.
(53) Wissel, K.; Heldt, J.; Groszewicz, P. B.; Dasgupta, S.; Breitzke, H.; Donzelli, M.; Waidha, A. I.; Fortes, A. D.; Rohrer, J.; Slater, P. R.; Buntkowsky, G.; Clemens, O. Topochemical Fluorination of La_2NiO_{4+d}: Unprecedented Ordering of Oxide and Fluoride Ions in $La_2NiO_3F_2$. *Inorg. Chem.* **2018**, *57*, 6549.
(54) Hancock, C. A.; Herranz, T.; Marco, J. F.; Berry, F. J.; Slater, P. R. Low temperature fluorination of $Sr_3Fe_2O_{7-x}$with polyvinylidine fluoride: An X-ray powder diffraction and Mössbauer spectroscopy study. *J. Solid State Chem.* **2012**, *186* (Supplement C), 195−203.
(55) Berry, F. J.; Heap, R.; Helgason, Ö.; Moore, E. A.; Shim, S.; Slater, P. R.; Thomas, M. F. Magnetic order in perovskite-related $SrFeO_2F$. *J. Phys.: Condens. Matter* **2008**, *20* (21), 215207.
(56) Seo, J. W.; Fullerton, E. E.; Nolting, F.; Scholl, A.; Fompeyrine, J.; Locquet, J. P. Antiferromagnetic $LaFeO_3$thin films and their effect on exchange bias. *J. Phys.: Condens. Matter* **2008**, *20* (26), 264014.
(57) Blakely, C. K.; Davis, J. D.; Bruno, S. R.; Kraemer, S. K.; Zhu, M.; Ke, X.; Bi, W.; Alp, E. E.; Poltavets, V. V. Multistep synthesis of the $SrFeO_2F$ perovskite oxyfluoride via the $SrFeO_2$infinite-layer intermediate. *J. Fluorine Chem.* **2014**, *159*, 8−14.
(58) Withers, R. L.; Brink, F. J.; Liu, Y.; Norén, L. Cluster chemistry in the solid state: Structured diffuse scattering, oxide/fluoride ordering and polar behaviour in transition metal oxyfluorides. *Polyhedron* **2007**, *26* (2), 290−299.
(59) Sturza, M.; Kabbour, H.; Daviero-Minaud, S.; Filimonov, D.; Pokholok, K.; Tiercelin, N.; Porcher, F.; Aldon, L.; Mentré, O. Unprecedented Robust Antiferromagnetism in Fluorinated Hexagonal Perovskites. *J. Am. Chem. Soc.* **2011**, *133* (28), 10901−10909.
(60) Clemens, O.; Marco, J. F.; Thomas, M. F.; Forder, S. D.; Zhang, H.; Cartenet, S.; Monze, A.; Bingham, P. A.; Slater, P. R.; Berry, F. J. Magnetic interactions in cubic-, hexagonal- and trigonal-barium iron oxide fluoride, $BaFeO_2F$. *J. Phys.: Condens. Matter* **2016**, *28* (34), 346001.
(61) Koehler, W. C.; Wollan, E. O. Neutron-diffraction study of the magnetic properties of perovskite-like compounds $LaBO_3$. *J. Phys. Chem. Solids* **1957**, *2* (2), 100−106.
(62) Alaria, J.; Borisov, P.; Dyer, M. S.; Manning, T. D.; Lepadatu, S.; Cain, M. G.; Mishina, E. D.; Sherstyuk, N. E.; Ilyin, N. A.; Hadermann, J.; Lederman, D.; Claridge, J. B.; Rosseinsky, M. J. Engineered spatial inversion symmetry breaking in an oxide heterostructure built from isosymmetric room-temperature magnetically ordered components. *Chem. Sci.* **2014**, *5* (4), 1599−1610.
(63) Zanolli, Z.; Wojdeł, J. C.; Íñiguez, J.; Ghosez, P. Electric control of the magnetization in $BiFeO_3/LaFeO_3$superlattices. *Phys. Rev. B: Condens. Matter Mater. Phys.* **2013**, *88* (6), 060102.
(64) Young, J.; Stroppa, A.; Picozzi, S.; Rondinelli, J. M. Tuning the ferroelectric polarization in $AA'MnWO_6$double perovskites through A cation substitution. *Dalton Trans.* **2015**, *44* (23), 10644−10653.
(65) Ecija, A.; Vidal, K.; Larrañaga, A.; Martínez-Amesti, A.; Ortega-San-Martín, L.; Arriortua, M. I. Characterization of $Ln_{0.5}M_{0.5}Fe_{O3-\delta}$(Ln = La, Nd, Sm; M = Ba, Sr) perovskites as SOFC cathodes. *Solid State Ionics* **2011**, *201* (1), 35−41.
(66) Antipov, E. V.; Abakumov, A. M.; Istomin, S. Y. Target-Aimed Synthesis of Anion-Deficient Perovskites. *Inorg. Chem.* **2008**, *47* (19), 8543−8552.
(67) Woodward, P. M.; Suard, E.; Karen, P. Structural Tuning of Charge, Orbital, and Spin Ordering in Double-Cell Perovskite Series between $NdBaFe_2O_5$and $HoBaFe_2O_5$. *J. Am. Chem. Soc.* **2003**, *125* (29), 8889−8899.
(68) Abakumov, A. M.; D'Hondt, H.; Rossell, M. D.; Tsirlin, A. A.; Gutnikova, O.; Filimonov, D. S.; Schnelle, W.; Rosner, H.; Hadermann, J.; Van Tendeloo, G.; Antipov, E. V. Coupled anion and cation ordering in $Sr_3RFe_4O_{10.5}$(R = Y, Ho, Dy) anion-deficient perovskites. *J. Solid State Chem.* **2010**, *183* (12), 2845−2854.
(69) Mishra, R.; Kim, Y.-M.; Salafranca, J.; Kim, S. K.; Chang, S. H.; Bhattacharya, A.; Fong, D. D.; Pennycook, S. J.; Pantelides, S. T.; Borisevich, A. Y. Oxygen-Vacancy-Induced Polar Behavior in $(LaFeO_3)_2/(SrFeO_3)$ Superlattices. *Nano Lett.* **2014**, *14* (5), 2694−2701.
(70) Young, J.; Moon, E. J.; Mukherjee, D.; Stone, G.; Gopalan, V.; Alem, N.; May, S. J.; Rondinelli, J. M. Polar Oxides without Inversion Symmetry through Vacancy and Chemical Order. *J. Am. Chem. Soc.* **2017**, *139* (7), 2833−2841.
(71) King-Smith, R. D.; Vanderbilt, D. Theory of polarization of crystalline solids. *Phys. Rev. B: Condens. Matter Mater. Phys.* **1993**, *47* (3), 1651−1654.
(72) Spaldin, N. A. A beginner's guide to the modern theory of polarization. *J. Solid State Chem.* **2012**, *195*, 2−10.
(73) Ong, S. P.; Richards, W. D.; Jain, A.; Hautier, G.; Kocher, M.; Cholia, S.; Gunter, D.; Chevrier, V. L.; Persson, K. A.; Ceder, G. Python Materials Genomics (pymatgen): A robust, open-source

DOI: 10.1021/acs.inorgchem.8b01253
Inorg. Chem. 2018, 57, 10616−10624

python library for materials analysis. *Comput. Mater. Sci.* **2013**, *68* (Supplement C), 314−319.
(74) Nowadnick, E. A.; Fennie, C. J. Domains and ferroelectric switching pathways in $Ca_2Ti_3O_7$from first principles. *Phys. Rev. B: Condens. Matter Mater. Phys.* **2016**, *94* (10), 104105.
(75) Shannon, R. D. Revised Effective Ionic-Radii and Systematic Studies of Interatomic Distances in Halides and Chalcogenides. *Acta Crystallogr., Sect. A: Cryst. Phys., Diffr., Theor. Gen. Crystallogr.* **1976**, *32* (Sep1), 751−767.
(76) Woodward, P. M. Octahedral Tilting in Perovskites. II. Structure Stabilizing Forces. *Acta Crystallogr., Sect. B: Struct. Sci.* **1997**, *53* (1), 44−66.
(77) Mulder, A. T.; Benedek, N. A.; Rondinelli, J. M.; Fennie, C. J. Turning ABO_3 Antiferroelectrics into Ferroelectrics: Design Rules for Practical Rotation-Driven Ferroelectricity in Double Perovskites and $A_3B_2O_7$ Ruddlesden-Popper Compounds. *Adv. Funct. Mater.* **2013**, *23* (38), 4810.
(78) May, S. J.; Kim, J. W.; Rondinelli, J. M.; Karapetrova, E.; Spaldin, N. A.; Bhattacharya, A.; Ryan, P. J. Quantifying octahedral rotations in strained perovskite oxide films. *Phys. Rev. B: Condens. Matter Mater. Phys.* **2010**, *82* (1), 014110.
(79) Zunger, A.; Wei, S. H.; Ferreira, L. G.; Bernard, J. E. Special quasirandom structures. *Phys. Rev. Lett.* **1990**, *65* (3), 353−356.
(80) van de Walle, A.; Tiwary, P.; de Jong, M.; Olmsted, D. L.; Asta, M.; Dick, A.; Shin, D.; Wang, Y.; Chen, L. Q.; Liu, Z. K. Efficient stochastic generation of special quasirandom structures. *CALPHAD: Comput. Coupling Phase Diagrams Thermochem.* **2013**, *42*, 13−18.
(81) El Shinawi, H.; Marco, J. F.; Berry, F. J.; Greaves, C. $LaSrCoFeO_5LaSrCoFeO_5F$ and $LaSrCoFeO_{5.5}$new La-Sr-Co-Fe perovskites. *J. Mater. Chem.* **2010**, *20* (16), 3253−3259.
(82) Raveau, B.; Caignaert, V.; Kundu, A. K. Double Cationic-Anionic Ordering in Ba-Based Oxygen-Deficient Perovskites. *Z. Anorg. Allg. Chem.* **2015**, *641* (6), 990−997.
(83) Sun, W.; Dacek, S. T.; Ong, S. P.; Hautier, G.; Jain, A.; Richards, W. D.; Gamst, A. C.; Persson, K. A.; Ceder, G. The thermodynamic scale of inorganic crystalline metastability. *Sci. Adv.* **2016**, *2* (11), e1600225.
(84) Saal, J. E.; Kirklin, S.; Aykol, M.; Meredig, B.; Wolverton, C. Materials Design and Discovery with High-Throughput Density Functional Theory: The Open Quantum Materials Database (OQMD). *JOM* **2013**, *65* (11), 1501−1509.
(85) Sanjaya Ranmohotti, K. G.; Josepha, E.; Choi, J.; Zhang, J.; Wiley, J. B. Topochemical manipulation of perovskites: low-temperature reaction strategies for directing structure and properties. *Adv. Mater.* **2011**, *23* (4), 442.
(86) Hayward, M. A. Topochemical reactions of layered transition-metal oxides. *Semicond. Sci. Technol.* **2014**, *29* (6), 064010.
(87) Clemens, O.; Haberkorn, R.; Slater, P. R.; Beck, H. P. Synthesis and characterisation of the $Sr_xBa_{1-x}FeO_{3-y}$system and the fluorinated phases $Sr_xBa_{1-x}FeO_2F$. *Solid State Sci.* **2010**, *12* (8), 1455−1463.
(88) Clemens, O.; Kuhn, M.; Haberkorn, R. Synthesis and characterization of the $La_{1-x}Sr_xFeO_{3-\delta}$system and the fluorinated phases $La_{1-x}Sr_xFeO_{3-x}F_x$. *J. Solid State Chem.* **2011**, *184* (11), 2870−2876.
(89) Clemens, O.; Berry, F. J.; Wright, A. J.; Knight, K. S.; Perez-Mato, J. M.; Igartua, J. M.; Slater, P. R. A neutron diffraction study and mode analysis of compounds of the system $La_{1-x}Sr_xFeO_{3-x}F_x$(x = 1, 0.8, 0.5, 0.2) and an investigation of their magnetic properties. *J. Solid State Chem.* **2013**, *206*, 158−169.

DOI: 10.1021/acs.inorgchem.8b01253
Inorg. Chem. 2018, 57, 10616−10624